

Imidazole Is a Sensitive Probe of Steric Hindrance in the Distal Pockets of Oxygen-Binding Heme Proteins[†]

Sheref S. Mansy,[‡] John S. Olson,[§] Gonzalo Gonzalez,^{||} and Marie A. Gilles-Gonzalez^{*,‡,||}

Ohio State Biochemistry Program, Department of Biochemistry, and Plant Biotechnology Center, The Ohio State University, 1060 Carmack Road, Columbus, Ohio 43210-1002, and Department of Biochemistry and Cell Biology and the W. M. Keck Center for Computational Biology, Rice University, 6100 Main Street, Houston, Texas 77005-1892

Received March 4, 1998

ABSTRACT: The FixL heme-based sensor, despite its low affinity for oxygen, is much more reactive than myoglobin toward the large polar ligand imidazole. To determine which features of a myoglobin heme pocket favor binding of imidazole, we have measured binding of this ligand to the FixL heme domain, elephant myoglobin, wild-type sperm whale myoglobin, and sperm whale myoglobins having alanine, valine, threonine, glutamine, leucine, phenylalanine, or tryptophan substitutions of the distal (E7) histidine residue. Except for histidine, the association rate constants dropped more than 3000-fold as the volume of the E7 side chain, at position 64, was expanded from alanine ($10^6 \text{ M}^{-1} \text{ s}^{-1}$) to phenylalanine ($10^3 \text{ M}^{-1} \text{ s}^{-1}$). There was inhibition of imidazole binding due to displacement of coordinated water from H64 and H64Q sperm whale myoglobins, where the E7 side chain hydrogen bonds directly to the bound ligand. The imidazole dissociation rate constants varied less dramatically and less consistently with any single factor, though they were measurably decreased by hydrogen bonding to an E7 glutamine or histidine. On the whole, the results for the sperm whale myoglobin E7 substitutions show that the rate constants for imidazole binding are useful and sensitive indicators of steric hindrance and polar interactions in the distal pockets of myoglobins. The combined effects of the glutamine 64 and phenylalanine 29 in elephant myoglobin largely account for its increased imidazole association and dissociation rate constants, respectively, compared to those of sperm whale myoglobin. An unhindered distal pocket not competent to stabilize positive poles is indicated by the large imidazole association ($\geq 10^4 \text{ M}^{-1} \text{ s}^{-1}$) and dissociation ($\geq 50 \text{ s}^{-1}$) rate constants, parameters that are characteristic of FixL.

A variety of heme proteins bind oxygen reversibly as part of their physiological functions. To accomplish this, the polypeptide must at least protect the heme prosthetic group from autoxidation and cause the protein-associated ferrous heme to discriminate much more strongly against carbon monoxide. In addition, the amino acid residues surrounding the heme iron have evolved to optimize the association and dissociation rates of oxygen so as to suit the physiological functions of the proteins. In hemoglobins and myoglobins, the two residues closest to the heme iron are the proximal (F8)¹ residue that coordinates directly to this atom and the

distal (E7) residue on the opposite side of the heme. Because of its proximity to the heme iron, the E7 side chain influences considerably the binding properties of the myoglobins, both by sterically controlling access to the iron atom and by stabilizing or destabilizing the bound ligand. For example, in most mammalian myoglobins, an E7 histidine, i.e., H64, stabilizes the highly polar iron–oxygen complex by hydrogen bonding (2).

Some myoglobins optimize their oxygen binding parameters by different mechanisms. For example, if the E7 histidine in SWMb is replaced by valine, the oxygen off rate constant increases more than 100-fold (3). Yet *Aplysia limacina* Mb naturally has an E7 valine and an off rate constant very similar to that of SWMb. In this protein, interactions with an E10 arginine stabilize the bound oxygen (4). In elephant Mb, an interaction of the positive edge of a B10 phenylalanine with the bound oxygen compensates for the substitution of the E7 histidine with the less effective hydrogen-bond donor glutamine (5–7). This combination of interactions results in similar oxygen affinity but 2-fold greater rate constants.

The distal pocket structure of FixL is unknown, but its visible and proton NMR spectra indicate the absence of hydrogen-bond acceptors near the ligand binding site (8, 9). Therefore other features of its heme pocket must be responsible for oxygen off rates similar to those of myoglo-

[†] Supported by National Science Foundation Grant MCB-9724048 (M.A.G.-G.), The Ohio State University (G.G.), U.S. Public Health Service Grants GM-35649 and HL-47020, Grant C-612 from the Robert A. Welch Foundation, and the W. M. Keck Foundation (J.S.O.).

* Corresponding author: Tel (614) 688-3303; Fax (614) 688-3302; E-mail gilles-gonzalez.1@osu.edu; web site <http://www.biosci.ohio-state.edu/~mgonzalez/MAGG.html>.

[‡] Ohio State Biochemistry Program.

[§] Rice University.

^{||} Department of Biochemistry, Plant Biotechnology Center, The Ohio State University.

¹ Abbreviations: RmFixLH, heme domain of *Rhizobium meliloti* FixL; Mb, myoglobin; SWMb, sperm whale myoglobin. The alphanumeric code (e.g., E7, B10) refers to the positions of amino acids in helices and turns of myoglobin and hemoglobin (1). Sperm whale myoglobin amino acid substitutions are described by the original residue, its position in the primary sequence, followed by the replacing residue; e.g., H64V denotes a change of the histidine at position 64 to a valine.

bins. Although ferrous FixL has an oxygen on rate constant that is over 60-fold slower than that of deoxySWMb, ferric FixL binds the much larger imidazole 70 times faster than metSWMb (8, 10). To understand this dramatic difference, we set out to determine which aspects of a heme pocket favor binding of imidazole. Site-directed mutagenesis makes it possible to engineer myoglobins with specific alterations to examine the effects of the polarity, size, and shape of the heme pocket (11–14).

Steric interference between the E7 residue and the bound imidazole was expected to be a major factor influencing the stability of binding. The crystal structures of the imidazole complexes for SWMb and *Aplysia* Mb have shown that the coordinated imidazole binds perpendicular to the plane of the heme, forcing the distal residue to move up from the heme iron and toward the solvent (4, 15). In SWMb, oxygen or imidazole can be stabilized by the E7 histidine, which can act as either a hydrogen-bond donor or acceptor. This stabilization does not occur in the myoglobins from mollusks such as *A. limacina* or *Dolabella auricularia*, which have an E7 valine. Crystallographic and proton NMR studies of their distal pockets have shown that while the guanidinium side chain of E10 arginine can donate a hydrogen to bound oxygen, it cannot accept a hydrogen from bound imidazole (4, 16).

The presence of coordinated water presents a kinetic barrier to ligand binding, since this water must be displaced before another ligand can bind. However, water is a very weak ligand that binds only when it is stabilized by interactions with nearby protein residues. In myoglobins with E7 histidine or glutamine, this stabilization occurs through direct hydrogen bonding. For those with E7 alanine or glycine, hydrogen-bond stabilization is weaker and occurs through a chain of water molecules leading from the solvent phase past the heme propionates to the iron atom (17). The coordinated water molecule position is partially occupied in the crystal structure of H64T SWMb. In the visible spectra, a narrow and intense absorption maximum near 408 nm is characteristic of ferric Mb having water at the sixth coordination position; a broad maximum near 395 nm is indicative of the pentacoordinate form that occurs in metMb with apolar distal side chains (17, 18). The absorption maximum for H64T metSWMb is 402 nm, which is intermediate between those characteristic of pentacoordinate and hexacoordinate heme. In metFixL and *A. limacina* metMb the ferric heme iron is clearly pentacoordinate, as indicated first by its absorption spectra and later by resonance Raman spectroscopy (8, 19).

It was of interest to understand the determinants of imidazole binding to myoglobins. We have examined the effects of size and polarity of the E7 side chain on binding of imidazole to a series of SWMb mutants and then used the results to interpret the imidazole binding properties of elephant Mb and the oxygen sensor FixL.

EXPERIMENTAL PROCEDURES

Preparation of Myoglobins. The *R. meliloti* FixL heme domain was prepared at The Ohio State University (8). Wild-type SWMb and the myoglobins having substitutions at position 64 were purified at Rice University from overexpressing strains of *Escherichia coli* harboring the

appropriate recombinant plasmids (3, 20, 21). Purified native elephant Mb was a gift of Dr. Jonathan Wittenberg of the Albert Einstein College of Medicine. The myoglobins were oxidized by equimolar potassium ferricyanide and then filtered through a Sephadex G25 column (Pharmacia) equilibrated with 20 mM Tris-HCl, pH 8.0, or 100 mM sodium phosphate, pH 7.0.

Affinities. Metmyoglobins (2.5–10 μ M) were titrated with increasing concentrations of imidazole. Isosbestic points were observed in the 350–700 nm region of the absorption spectra. Entire spectra were used for the K_d determination. The absorption spectra were decomposed by multiple linear regression analysis into the proportions of the liganded and unliganded species. The fraction of the liganded species was taken as the saturation. Values of n and of K_d were obtained from Hill plots (22).

Association Rate Constants. Imidazole concentrations were chosen to give the widest measurable range of speeds. As a rule, the ligand concentrations ranged from below to above the K_d . The rates of imidazole binding were measured with an Applied Photophysics SX17MV reaction analyzer (Leatherhead, U.K.). The reactions were followed at the wavelength of maximal difference between the unliganded and the liganded species of Mb at pH 8.0, 25 °C. Those difference maxima were at 418 nm (absorbance increase as imidazole binds) for most of the proteins and at 405 nm for elephant Mb (absorbance decrease as imidazole binds). Variations between the difference spectra were due not to the bis-imidazole complexes but to the different proportions of the aquomet form in the different proteins (7, 17). The static absorption spectra were measured with an ATI Unicam UV4 UV-Vis spectrophotometer.

Solutions of imidazole were prepared in the same buffer as the protein (20 mM Tris-HCl, pH 8.0, or 100 mM sodium phosphate, pH 7.0). The concentration of protein in the stopped-flow syringe was 5 μ M, except for H64A SWMb and elephant Mb, which were at 2.5 μ M. For each imidazole concentration a time course was measured at least three times, and the k_{obs} was computed from the average. All of the time courses were fit to a single exponential. The association rate constants were computed from the slopes of the linear portion of plots of k_{obs} versus the imidazole concentration. These lines usually included points at 5–7 ligand concentrations and had $r^2 > 0.99$. Activation energies were determined from Arrhenius plots of rate constants measured at 6, 10, 15, 25, and 37 °C in 100 mM sodium phosphate, pH 7.0; all other rate measurements were at 25 °C.

Dissociation Rate Constants. The dissociation rate constants of imidazole were determined by ligand replacement methods (10, 23, 24). High concentrations of cyanide (the displacing ligand) were added to the ferric heme proteins after they had been saturated with imidazole in 100 mM sodium phosphate, pH 7.0. The displacement reactions were followed at 430 nm, the wavelength of maximal difference between the imidazolylmet and cyanomet species.

RESULTS

Influence of Steric Hindrance and Water Displacement on the Association Rate Constants. Figure 1A displays the inverse exponential relationship between the size of the E7

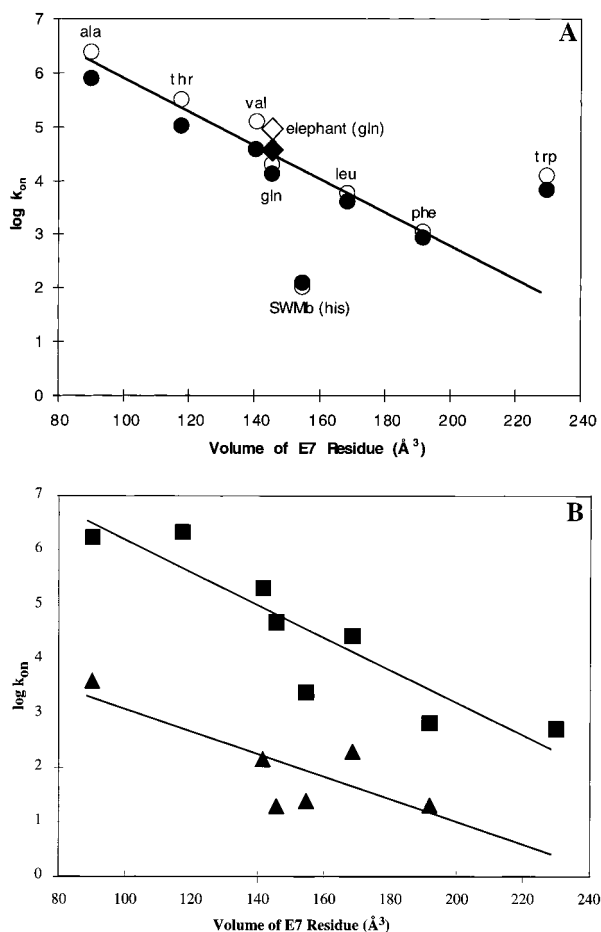


FIGURE 1: Influence of the bulk of the E7 residue on the rates of ligand association to myoglobins. The imidazole association rate constants were determined from time courses measured shortly after the met species were mixed with varying concentrations of that ligand in a stopped-flow rapid-mixing spectrometer. (Details are in Experimental Procedures.) The volumes of the amino acid side chains are from Creighton (30). Unless otherwise noted, the amino acid residues refer to substitutions of the E7 histidine (H64) of SWMb. Panel A shows binding of imidazole to SWMb (circles) and elephant Mb (diamonds). Panel B shows binding of azide (squares) and *n*-butyl isocyanide (triangles) to SWMb (3). Association rate constants were determined at pH 7.0 (closed symbols) and pH 8.0 (open symbols).

residue and the association rate constant for binding of imidazole at pH 7.0 and 8.0. Similar overall trends have been observed for the entry of azide and *n*-butyl isocyanide into heme pockets, with the k_{on} values dropping more than 3000-fold as the volume of the distal side chain is expanded less than 3-fold (Figure 1B) (3, 24). In contrast, the association rate constants for oxygen and carbon monoxide binding are virtually independent of the size of the E7 residue (25). This suggests that the E7 residue presents a considerable steric barrier to bulky ligands. Nonetheless, there remain some interesting differences in the ways heme pockets accommodate each large ligand. For example, lengthening the E7 side chain in SWMb by one carbon, from valine to leucine, did decelerate the on rate of imidazole 10-fold and that of azide 8-fold, but it slightly accelerated the association of *n*-butyl isocyanide. Although the indole side chain of an E7 tryptophan impeded the entry of azide even more, the presence of this bulky group appears to facilitate imidazole binding.

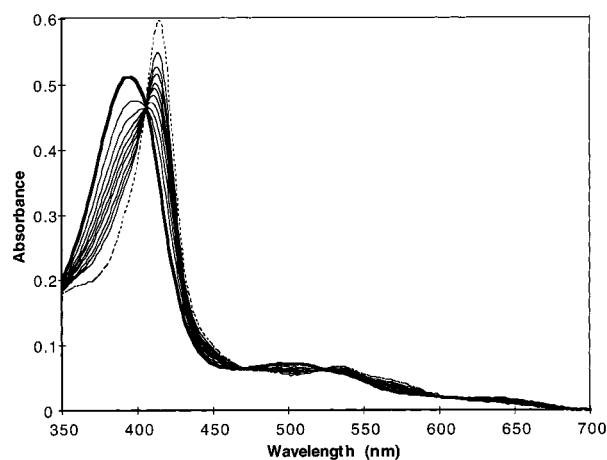


FIGURE 2: Binding of imidazole at 25 °C and pH 8.0 to a ferric sperm whale myoglobin having an E7 substitution. The conversion of H64V metSWMb (thick line) to H64V imidazolylmet SWMb (broken lines) is shown. The equilibrium dissociation constants at pH 8.0 listed in Table 1 were determined from similar titrations.

The largest imidazole association rate constant, $1 \times 10^6 \text{ M}^{-1} \text{ s}^{-1}$ was observed for H64A SWMb. Even though water is coordinated to the iron atom in H64A metSWMb, its displacement does not confer much resistance to imidazole binding. The rate constant for completely pentacoordinate H64V metSWMb is actually 10-fold smaller than that for the H64A metSWMb. The opposite effect is observed for oxygen binding. The association rate constant for oxygen binding to H64A deoxySWMb is roughly half that for the H64V deoxySWMb. Even more surprising, H64T metSWMb, which is isosteric with H64V but contains coordinated water, has a 2-fold greater association rate constant for imidazole binding and 10-fold greater rate constant for azide binding.

Factors Affecting the Dissociation Rate Constants. The relationship between the E7 residue of Mb and the imidazole dissociation rate constant is much more complex, involving a combination of polarity and steric hindrance effects. E7 side chains such as alanine, threonine, glutamine, or histidine, that permit hydrogen bonding to bound ligands, whether directly or via a molecule of water, correlate roughly with lower dissociation rate constants for both oxygen and imidazole binding (Table 1) (17). This hydrogen-bonding stabilization is most apparent in the 10-fold differences between k_{off} for imidazole dissociation from H64T and H64V metSWMb and between wild-type (H64) and H64F metSWMb. Steric factors also seem to have considerable influence on imidazole dissociation. For example, increasing the size of the distal side chain from valine to leucine reduces the k_{off} for imidazole 25-fold.

Equilibrium Constants. Figure 2 shows the titration of H64V metSWMb with imidazole. Whether the metmyoglobins were pentacoordinate or aquomet, their imidazole complexes were identical. FixL, elephant Mb, SWMb, and all the SWMb mutants had their imidazolylmet Soret peak at 415 nm and their β -peak at 535 nm. As expected, the binding of imidazole was noncooperative, with a Hill constant of 1. The highest affinities at pH 8.0 were observed for H64A, H64Q, and H64T metSWMb, which showed equilibrium dissociation constants equal to 7.5, 12, and 44 μM , respectively (Table 1). For each of these proteins, large association rate constants were augmented by their relatively small dissociation rate constants. The large association rate

Table 1: Rate and Equilibrium Parameters for Binding of Imidazole to Heme Proteins at 25 °C^a

protein	k_{on} (M ⁻¹ s ⁻¹)	k_{off} (s ⁻¹)	K_{d} (mM)	E_{a}^{on} (kcal/mol)	A^{on} (M ⁻¹ s ⁻¹)
pH 7.0					
H64A SWMb	1.0×10^6	17	0.017		
H64T SWMb	1.3×10^5	12	0.089	19	8.3×10^{18}
H64V SWMb	5.4×10^4	120	2.2	17	8.0×10^{16}
H64Q SWMb	1.7×10^4	0.9	0.053	17	4.6×10^{16}
H64 SWMb, wild type	1.6×10^2	3.6	22	17	3.2×10^{14}
H64L SWMb	5.2×10^3	4.7	0.91		
H64F SWMb	1.1×10^3	43	39		
H64W SWMb	8.4×10^3	19	2.3		
Q64/F29 elephant Mb, native	3.6×10^4	53 ^b	1.5		
H64/L29 SWMb, wild type	1.6×10^2	3.6	22		
H64Q/L29 SWMb	1.7×10^4	0.9	0.053		
H64/L29F SWMb	1.2×10^2	44 ^b	370		
H64Q/L29F SWMb	4.0×10^4	19 ^b	0.48		
RmFixLH	1.6×10^4	94 ^b	5.9	20	3.8×10^{18}
pH 8.0					
H64A SWMb	4.0×10^6	30	0.0075		
H64T SWMb	4.1×10^5	18	0.044		
H64V SWMb	1.5×10^5	72	0.48		
H64Q SWMb	2.5×10^4	0.30	0.012		
H64 SWMb, wild type	1.3×10^2	3.7	28		
H64L SWMb	7.3×10^3	5.1	0.7		
H64F SWMb	1.4×10^3	50	36		
H64W SWMb	1.5×10^4	54	3.6		
Q64/F29 elephant Mb, native	9.2×10^4	26	0.28		
H64/L29 SWMb, wild type	1.3×10^2	3.7	28		
RmFixLH ^c	5.0×10^4	100	2.0		

^a Unless otherwise noted, k_{on} and k_{off} listed for pH 7.0 were measured directly, and K_{d} was calculated as $k_{\text{off}}/k_{\text{on}}$; the parameters listed for pH 8.0 represent directly measured k_{on} and K_{d} and calculations of the k_{off} as $K_{\text{d}}k_{\text{on}}$. The time courses of association were measured by mixing the met proteins with various concentrations of imidazole and following the absorption at the wavelength of maximal difference between the met and imidazolylmet species in a stopped-flow rapid-mixing spectrometer. The time courses of imidazole dissociation were measured by following the replacement of bound imidazole by cyanide at 430 nm (23). The direct measurements of K_{d} were done by titrating the met species with imidazole. ^b Obtained by extrapolating the apparent on rates to zero ligand. ^c Winkler et al. (26).

constants for these mutants must be due to significantly less steric hindrance by the smaller or more flexible E7 side chains, while the lower dissociation rate constants appear to be due to stabilization of the bound ligand by either direct polar interactions or intervening water molecules. The lowest affinities were observed for the wild-type and H64F metSWMb, which showed equilibrium dissociation constants of 28 000 and 36 000 μM , respectively. Despite hydrogen-bond stabilization of the bound ligand, the affinity of wild-type metSWMb is reduced markedly by an abnormally low association rate constant, showing that steric hindrance by the large histidyl side chain is the dominant factor regulating the equilibrium binding of imidazole. This interpretation is supported by the low affinity of H64F metSWMb for imidazole. In the latter case, the large benzyl side chain sterically hinders access to the iron atom without providing electrostatic stabilization of the bound ligand.

Comparisons with Naturally Occurring Myoglobins. While SWMb has an E7 histidine and a B10 leucine, elephant Mb has an E7 glutamine and a B10 phenylalanine (6, 7). Compared to wild-type SWMb, the H64Q substitution causes a 100-fold increase in the imidazole association rate constant, whereas the L29F substitution causes a more than 10-fold increase in the dissociation rate constant (Table 1). The introduction of both mutations, i.e., H64Q/L29F SWMb, results in kinetic parameters for imidazole binding more comparable to those of elephant Mb.

Table 1 shows clearly that the association rate constant for imidazole binding is governed primarily by steric factors.

Thus the large association rate constant for imidazole binding to FixL supports the assertion that the distal cavity of this protein is relatively unhindered (26). The large dissociation rate constant indicates that there is little hydrogen-bond stabilization of the bound imidazole in FixL. Overall, the kinetic parameters for imidazole binding to metFixL most closely resemble those of elephant metMb and H64V metSWMb. For both of these proteins, relatively small or flexible E7 side chains permit the rapid entry of imidazole, and there appears to be little significant stabilization of the bound ligand. Although the distal cavity in FixL readily accommodates imidazole, the heme domain of the *R. meliloti* FixL still discriminates in favor of oxygen and against carbon monoxide to almost the same extent as wild-type SWMb (8). This result suggests that there may be auxiliary polar interactions on the distal side of the heme group in FixL, since the M values of Mb mutants containing completely apolar distal pockets are very large, 10 000–50 000 (14).

DISCUSSION

Steric Hindrance by the E7 Side Chain. The three-dimensional structures of imidazolylmet-SWMb and *Aplysia* Mb indicate that the imidazole binds in a plane approximately perpendicular to the porphyrin ring (4, 15, 27). In available structures for myoglobins with an E7 histidine, this residue is positioned above the heme iron with the ring plane also approximately perpendicular to the heme. Therefore, it seemed likely that this residue would pose considerable hindrance to the entry of imidazole. Our results show that

the most influential factor in the binding of imidazole to Mb is indeed steric hindrance. This is fundamentally unlike the binding of oxygen and carbon monoxide. For these smaller ligands of ferrous heme, the displacement of water from the distal pocket poses an important kinetic barrier, whereas the size of the distal side chain is less important (25). In contrast, an approximately 3-fold reduction in the volume of the E7 side chain results in a 3000-fold increase of the association rate constant for binding of imidazole (Table 1, Figure 1). A similar large effect of the size of the E7 residue has been observed for azide binding, but this ligand is charged in addition to being larger than oxygen (24). Significant but less dramatic increases in association rate constants with decreasing size of residue E7 were observed for methyl, ethyl, *n*-propyl, and *n*-butyl isocyanide binding to deoxy-SWMB (3). Thus imidazole can also be used as a simple and sensitive probe of steric hindrance in the distal heme pockets of myoglobins.

The logarithmic relationship between the size of the distal residue and the imidazole on rate constants suggests an activation free energy barrier that is proportional to the size of the distal side chain. Interestingly, identical activation energies are observed for imidazole binding to wild-type, H64V, and H64Q metSWMBs despite their considerably different k_{on} values (Table 1). The correlation of the rate constants with the Arrhenius amplitudes, A , indicate that entropic effects are more influential. Those effects likely reflect the difficulties that imidazole encounters in achieving the proper orientation for binding to the heme iron. Larger E7 side chains would impede this process considerably more than smaller ones.

Given that crowding of the heme pocket dramatically interferes with the rate of imidazole binding, how then does this ligand bind more rapidly to H64W metSWMB than to H64F metSWMB? Perutz and Mathews (28) have proposed a model for ligand entry in which the E7 histidine functions as a swinging gate that occasionally allows the ligand to enter. Indeed, binding of imidazole or ethyl isocyanide causes this residue to swing toward the protein surface, into the "open conformation" (27, 29). The swinging-gate model would predict that if the E7 residue is replaced with increasingly larger side chains, a size may be reached that will not allow the "gate" to close. The data in Figure 2 indicate that E7 phenylalanine SWMB can adopt the closed conformation, whereas E7 tryptophan allows more rapid entry of imidazole.

Influence of Water and Polar Interactions. Displacement of water from the ferric heme iron poses a less significant barrier to imidazole binding than steric factors. Indeed, small polar E7 side chains aid the entry of this ligand. For example, imidazole as well as azide bind more rapidly to the H64T than to the H64V metSWMB, although the former is predominantly in the aquomet form, and the latter is pentacoordinate (Table 1). Brancaccio and his colleagues (24) have suggested that a polar channel involving the E7 threonine facilitates the entry of azide into the heme pocket. Such a channel could also favor imidazole and other polar ligands. Polar E7 side chains clearly stabilize the imidazole once it is bound. The stabilizing impact of polar interactions is readily illustrated by the 10-fold slower dissociation of imidazole from H64T compared to H64V metSWMB at pH 7.0. Similarly, the more than 10-fold slower dissociation

of imidazole from the wild-type compared to H64F metSWMB is due to polar interactions.

Implications for Other Oxygen Binding Heme Proteins. The heme pocket of elephant Mb differs from that of SWMB at several positions. Of these differences the E7 glutamine and B10 phenylalanine have the most significant effect on reactions with ligands of ferrous heme (6, 7). The smaller and more flexible E7 glutamyl side chain of elephant metMb largely accounts for its larger imidazole association rate constant compared to that of metSWMB. For H64Q SWMB, H64Q/L29F SWMB, and elephant Mb, the imidazole association rate constants are comparable, i.e., $10^4 \text{ M}^{-1} \text{ s}^{-1}$. This represents a 100-fold increase compared to SWMB. The increase in the dissociation rate constant for elephant Mb is due to the additional presence of a B10 (i.e., residue 29) phenylalanine instead of a leucine (Table 1). The large benzyl side chain sterically hinders the bound imidazole, increasing its rate of dissociation. This phenomenon was observed for ethyl isocyanide binding to deoxySWMB, where the L29F substitution caused an approximately 15-fold increase in the rate of dissociation of this large ligand, with little or no effect on the association rate constant (21).

For metFixL, unlike metMb, there is a strong correlation between the association rates of ligands and their pK_a values, which reflect the tendency of the ligands to donate electrons (26). This indicates that, for FixL, formation of the coordinate bond between the heme iron and the ligand dominates the kinetics of association. The results in Table 1 and Figure 1 leave little doubt that the FixL protein has an unhindered distal pocket. Thus the very small oxygen and carbon monoxide association rates of FixL are due not to steric hindrance but rather to the intrinsic reactivity of the heme iron. This reactivity is strongly influenced by the iron-F8 histidine bond, which has a trans effect on coordination of the external ligand.

In most vertebrate myoglobins, an E7 histidine or glutamine functions as a hydrogen-bond donor during its interactions with the negative pole of oxygen bound to ferrous heme iron. For the same side chain to interact with the hydrogen atoms of H_2O bound to ferric heme iron, they must also be competent to function as hydrogen-bond acceptors. Comparison of the ligand dissociation rates indicate a stabilizing interaction in FixL quite different from that of vertebrate myoglobins. Absorption spectra and resonance Raman spectra show that ferric FixL is pentacoordinate and without an aquomet form (8, 19). This failure to coordinate water reflects a lack of effective stabilization by a hydrogen-bond acceptor like an E7 histidine or glutamine. The relatively large imidazole dissociation rate of FixL is also consistent with the absence of stabilization by a hydrogen-bond accepting distal side chain (Table 1). Nonetheless oxygen is undoubtedly stabilized in FixL, as revealed by oxygen dissociation rate constants that are comparable to those of myoglobins (8). Unlike the E7 histidine in SWMB that can stabilize either the positive or negative end of a dipole, the interactions in FixL seem to stabilize only negative poles, such as the one in bound oxygen. This is more reminiscent of the E10 arginine in *Aplysia* Mb or the B10 phenylalanine in elephant Mb. While a guanidinium side chain or the positive edge of phenylalanine can stabilize bound oxygen, it is not competent to stabilize bound H_2O or imidazole.

ACKNOWLEDGMENT

We thank Dr. Jonathan B. Wittenberg for his kind gift of purified elephant Mb and T. Patrick Purk for stimulating discussions throughout the course of this work.

REFERENCES

1. Perutz, M. F. (1970) *Nature* 228, 726–739.
2. Philips, S. E. V., and Schoenborn, B. P. (1981) *Nature* 292, 81–82.
3. Rohlfs, R. J., Mathews, A. J., Carver, T. E., Olson, J. S., Springer, B. A., Egeberg, K. D., and Sligar, S. G. (1990) *J. Biol. Chem.* 265, 3168–3176.
4. Conti, E., Moser, C., Rizzi, M., Mattevi, A., Lionetti, C., Coda, A., Ascenzi, P., Brunori, M., and Bolognesi, M. (1993) *J. Mol. Biol.* 233, 498–508.
5. Cupane, A., Leone, M., Vitrano, E., Cordone, L., Hiltbold, U. R., Winterhalter, K. H., Yu, W., and Di Iorio, E. E. (1993) *Biophys. J.* 65, 2461–2472.
6. Bisig, D. A., Di Iorio, E. E., Diederichs, K., Winterhalter, K. H., and Piontek, K. (1995) *J. Biol. Chem.* 270, 20754–20762.
7. Zhao, X., Vyas, K., Nguyen, D., Rajarathnam, K., la Mar, G. N., Li, T., Phillips, G. N., Eich, R. F., Olson, J. S., Ling, J., and Bocian, D. F. (1995) *J. Biol. Chem.* 270, 20763–20774.
8. Gilles-Gonzalez, M. A., Gonzalez, G., Perutz, M. F., Kiger, L., Marden, M. C., and Poyart, C. (1994) *Biochemistry* 33, 8067–8073.
9. Bertolucci, C., Ming, L. J., Gonzalez, G., and Gilles-Gonzalez, M. A. (1996) *Chem. Biol.* 3, 561–566.
10. Antonini, E., and Brunori, M. (1971) *Hemoglobin and Myoglobin in Their Reactions With Ligands*, American Elsevier Publishing Co., New York.
11. Nagai, K., Perutz, M. F., and Poyart, C. (1985) *Proc. Natl. Acad. Sci. U.S.A.* 82, 7252–7255.
12. Varadarajan R., Szabo, A., and Boxer S. G. (1985) *Proc. Natl. Acad. Sci. U.S.A.* 82, 5681–5684.
13. Springer, B. A., and Sligar, S. G. (1987) *Proc. Natl. Acad. Sci. U.S.A.* 84, 8961–8965.
14. Springer, B. A., Sligar, S. G., Olson, J. S., and Phillips, G. N., Jr. (1994) *Chem. Rev.* 94, 699–714.
15. Lionetti, C., Guanziroli, M. G., Frigerio, F., Ascenzi, P., and Bolognesi, M. (1991) *J. Mol. Biol.* 217, 409–412.
16. Yamamoto, Y., Suzuki, T., and Hori, H. (1995) *Biochim. Biophys. Acta* 1248, 149–158.
17. Quillin, M. L., Arduini, R. M., Olson, J. S., and Phillips, G. N., Jr. (1993) *J. Mol. Biol.* 234, 140–155.
18. Shikama, J., and Matsuoka, A. (1989) *J. Mol. Biol.* 209, 489–491.
19. Rodgers, K. R., Lukat-Rodgers, G. S., and Barron, J. A. (1996) *Biochemistry* 35, 9539–9548.
20. Egeberg, K. D., Springer, B. A., Sligar, S. G., Carver, T. E., Rohlfs, R. J., and Olson, J. S. (1990) *J. Biol. Chem.* 265, 11788–11795.
21. Carver, T. E., Brantley, R. E., Jr., Singleton, E. W., Arduini, R. M., Quillin, M. L., Phillips, G. N., Jr., and Olson, J. S. (1992) *J. Biol. Chem.* 267, 14443–14450.
22. Hill, R., and Wolvekamp, H. P. (1936) *Proc. R. Soc. London B* 120, 484.
23. Olson, J. S. (1981) *Methods Enzymol.* 76, 631–651.
24. Brancaccio, A., Cutruzzola, F., Allocatelli, C. T., Brunori, M., Smerdon, S., Wilkinson, A. J., Do, Y., Keenan, D., Ikeda-Saito, M., Brantley, R. E., Jr., and Olson, J. S. (1994) *J. Biol. Chem.* 269, 13843–13853.
25. Olson, J. S., and Phillips, G. N., Jr. (1997) *J. Biol. Inorg. Chem.* 2, 544–552.
26. Winkler, W. C., Gonzalez, G., Wittenberg, J. B., Hille, R., Dakappagari, N., Jacob, A., Gonzalez, L. A., and Gilles-Gonzalez, M. A. (1996) *Chem. Biol.* 3, 841–850.
27. Bolognesi, M., Cannillo, E., Ascenzi, P., Giacometti, G. M., Merli, A., and Brunori, M. (1982) *J. Mol. Biol.* 158, 305–315.
28. Perutz, M. F., and Mathews, F. S. (1966) *J. Mol. Biol.* 21, 199–202.
29. Johnson, K. A., Olson, J. S., and Phillips, G. N. (1989) *J. Mol. Biol.* 207, 459–463.
30. Creighton, T. E. (1984) *Proteins: Structures and Molecular Properties*, p 7, W. H. Freeman and Co., New York.

BI980516J